

Supporting Information
Nanopore analysis of individual RNA/antibiotic complexes

Meni Wanunu, Swati Bhattacharya, Yun Xie, Yitzhak Tor, Aleksei Aksimentiev, and Marija Drndic

I. Fluorescence titration curves of a A-site analogue with aminoglycosides

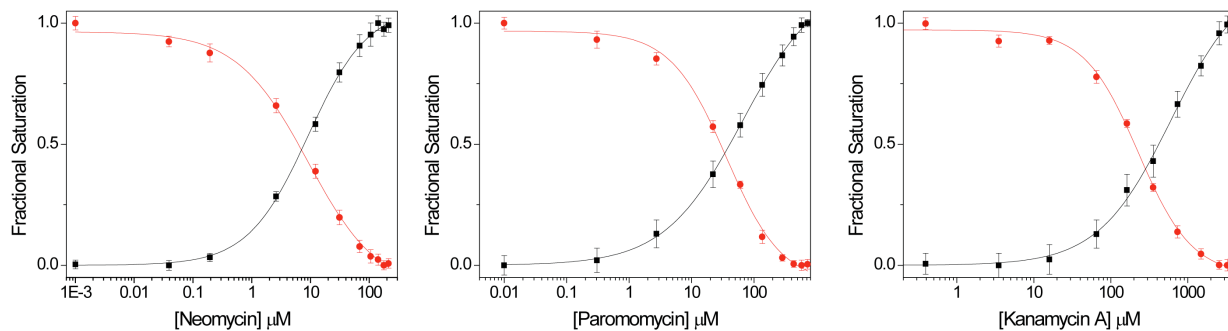


Figure S1. Fractional fluorescence saturation of the donor (■) in the labeled A-site and the emissive acceptor (●) in the coumarin labeled kanamycin A in studying the binding of neomycin, paromomycin, and kanamycin A. Conditions: Labeled A-site (1.0×10^{-6} M), cacodylate buffer pH 8.0 (2.0×10^{-2} M), NaCl (0.5 M), EDTA (5.0×10^{-4} M).

Table S1. IC₅₀ Values of antibiotics for the labeled A-site.^a

Antibiotic	16S A-Site (10^{-6} M)
Neomycin	7 (\pm 1)
Paromomycin	33 (\pm 4)
Kanamycin A	270 (\pm 10)

^a Conditions as listed in Figure S1.

All titrations were performed with working solutions of 1.0×10^{-6} M labeled A-site in 20×10^{-6} M cacodylate buffer (pH 8.0, 5.0×10^{-1} M NaCl, 5.0×10^{-4} M EDTA). The solutions were heated to 75 °C for 5 min, cooled to room temperature over 2 h, and placed on ice for 30 min prior to titrations. Coumarin-labeled kanamycin A was first titrated into the RNA, and unlabeled antibiotics were then titrated into the FRET-based RNA–ligand complex as reported (Figure S2).^{1,2} The solution was excited at 320 nm, and changes in emission upon displacement of coumarin-labeled kanamycin A by unlabeled paromomycin were monitored at 395 nm and 473 nm. IC₅₀ values were calculated using OriginPro 8 software by fitting a dose response curve to the fractional fluorescence saturation plotted against the log of antibiotic concentration.

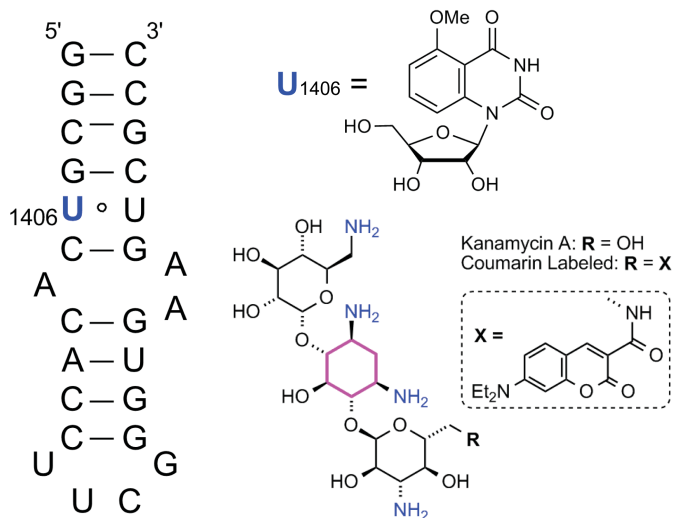


Figure S2. Labeled 16S A-site and coumarin-labeled kanamycin A used in FRET experiments.

See Ref. 1 for the synthesis of labeled 16S A-site and Ref. 2 for the synthesis of the coumarin-labeled kanamycin A. Unlabeled 16S A-site was purchased from Integrated DNA Technologies. The RNA was purified by gel electrophoresis and desalting on a Sep-Pak (Waters Corporation). Paromomycin and kanamycin A sulfate salts were purchased from Sigma-Aldrich and were converted into the corresponding neutral form by passing through DOWEX® MONOSPHERE® 550 Å (OH) anion exchange resin.

References

1. Xie, Y.; Dix, A. V.; Tor, Y. *J. Am. Chem. Soc.* **2009**, *131*, 17605–17614.
2. Xie, Y.; Dix, A. V.; Tor, Y. *Chem. Commun.* **2010**, *46*, 5542–5544.

II. Prolonged ion current trace through a nanopore during a typical experiment

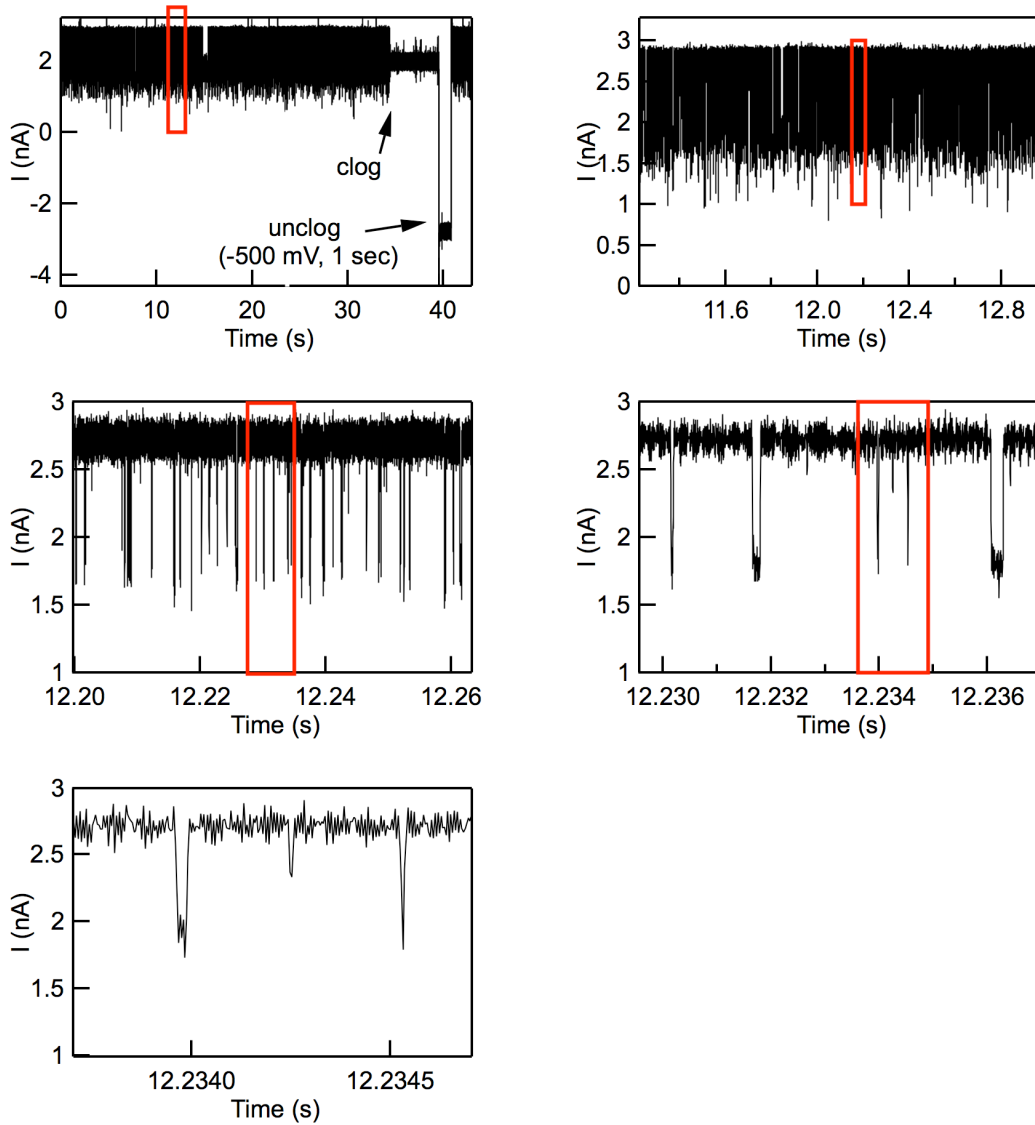
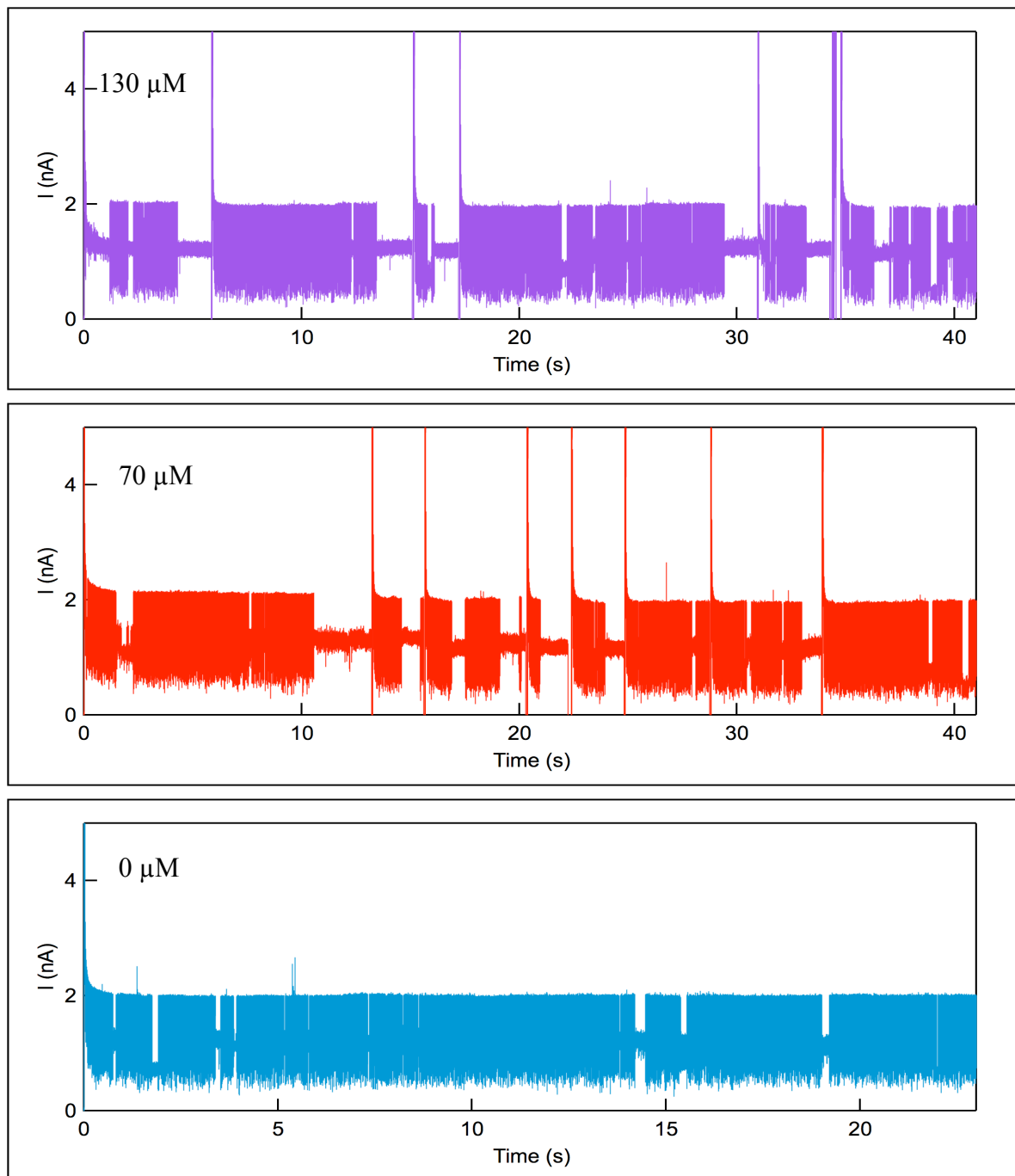


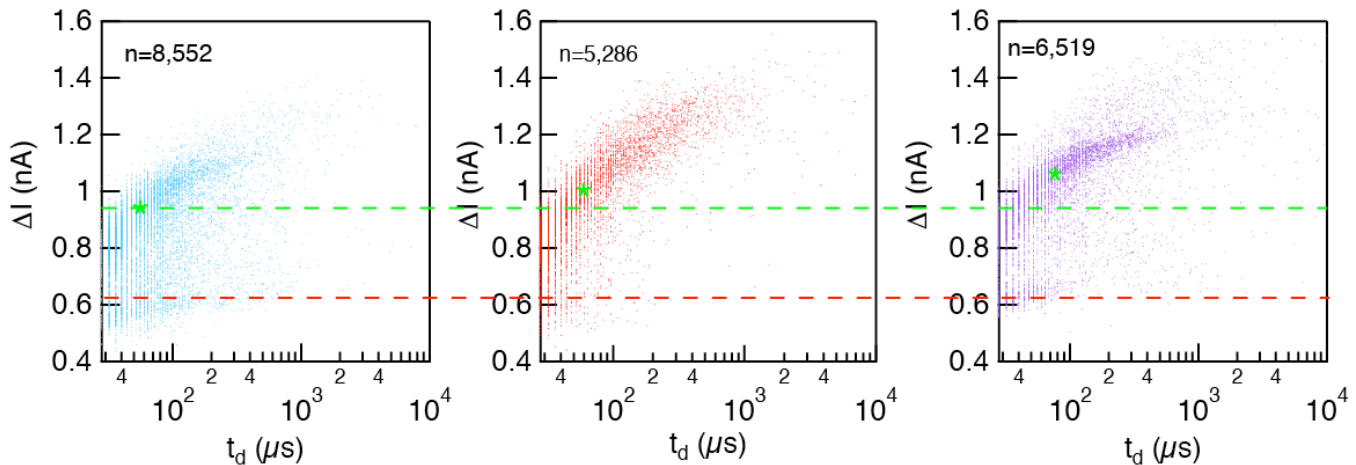
Figure S3. Continuous, 43-second trace of the ion current through a 3 nm-diameter pore under a 500 mV applied voltage and at 0°C following the addition of 1 μ M A-site RNA to the sample chamber. The series of images that progressively show zoomed-in regions of the trace reveal that the signal is composed of discrete downward spikes, mostly similar in their amplitude (0.9-1.0 nA). Occasional clogging of the molecule is reversed by briefly reversing the voltage applied to the pore.

III. Continuous traces and scatter plots of A-site titration with paromomycin

Figure S4. S4-a) Continuous current data recordings obtained during the titration of 1 μM A-site with PM at concentrations of 0 μM , 70 μM , and 130 μM . Sample data of durations of 20-40 sec were collected for each concentration, and three representative concentrations are shown that correspond to Figure 2. Occasionally during data collection a molecule got stuck at the pore mouth, reducing the open pore current by ~ 0.6 nA. Transient reversal and restoration of the voltage (indicated by negative followed by positive current spikes) restores a functional pore. Data for calculation of mean ΔI values was obtained by analyzing a net ~ 10 seconds of current data in which there are no long-lived obstructions of the pore (these singularities were cut out prior to analysis).



S4-b) Current amplitude vs. dwell-time scatter plots for titration of A-site with paromomycin, at points that correspond to the data in Figure 2b of the paper. Based on previous data and results obtained using protein pores (e.g., see Vercoutere et al., Nature Biotechnology 2001 for hairpins stuck in the entrance of α -hemolysin pore; or Wanunu et al. Biophysical Journal 2008 for 400 bp DNA molecules in 4 nm solid-state nanopores, as well as other papers), we hypothesize that the red and green dashed lines correspond to collisions and translocations of the RNA through the pore, respectively. The green asterisks drawn in each population represent the mean current amplitude of the translocation events (we exclude collision events from the analysis by eliminating all events with current amplitudes of less than 0.7 nA, as determined by a minimum in the all-point histograms in Figure 2b of the MS).



Triple-Gaussian Fit parameters for Figure 2 (green curves):

$$f(x) = a_1 * \exp(-((x-x_1)/w_1)^2) + a_2 * \exp(-((x-x_2)/w_2)^2) + a_3 * \exp(-((x-x_3)/w_3)^2)$$

0 μM (double-Gaussian fit*):	70 μM:	130 μM:
a1=95.386 ± 1.62	a1=20.052 ± 2.48	a1=63.066 ± 2.87
a2 = 207.77 ± 0.956	a2=101.27 ± 4.59	a2=121.79 ± 1.88
a3 = 0.00 ± 0	a3=67.299 ± 6.84	a3=71.407 ± 3.13
x1 = 0.59628 ± 0.00103	x1=0.6007 ± 0.00759	x1=0.62779 ± 0.00177
x2 = 0.90361 ± 0.000844	x2=0.90114 ± 0.0129	x2=0.99589 ± 0.00347
x3 = 0.00 ± 0	x3=1.1591 ± 0.018	x3=1.1317 ± 0.00197
w1 = 0.07166 ± 0.00153	w1=0.069675 ± 0.011	w1=0.047778 ± 0.00261
w2 = 0.20039 ± 0.00134	w2=0.17407 ± 0.0131	w2=0.23857 ± 0.00351
w3 = 0.01 ± 0	w3=0.1609 ± 0.0132	w3=0.064009 ± 0.00347

*Values highlighted in red were manually imposed to effectively provide a double-Gaussian fit for pure A-site RNA only.

IV. Stability of the molecular models in MD simulations

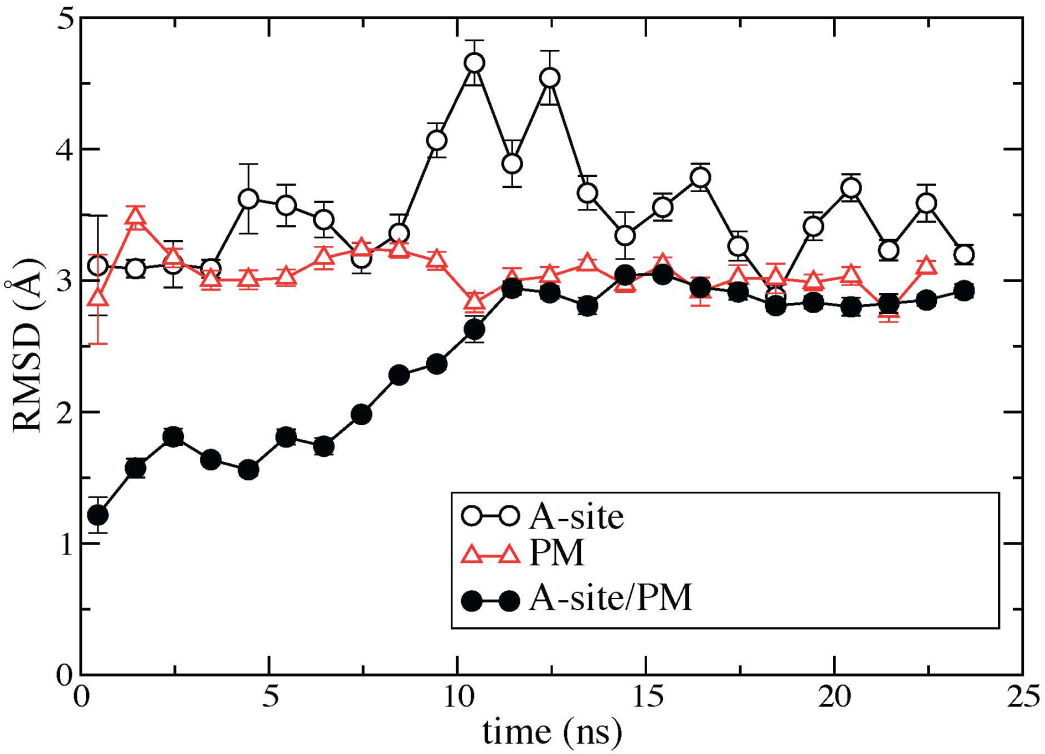


Figure S5: Stability of the all-atom models in MD simulations. The root mean square deviation (RMSD) of the heavy atoms of the A-site RNA, PM and A-site/PM complex from their respective NMR coordinates (PDB entry code 1PBR) is plotted versus time during free equilibration at 295 K. The RMSD data are block-averaged using a 1-ns window.

To assess the stability of our MD models of the A-site, PM and the A-site/PM complex, each molecule was simulated in 1M KCl solution at 295K in the absence of the solid-state membrane and the external electric field. The systems used for these simulations contained either 3991 or 6449 water molecules for the PM or A-site and A-site/PM models, respectively. The systems were first minimized for 1800 steps and then equilibrated at 295 K at constant pressure of 1 bar. During the constant pressure equilibration, harmonic restraints were applied to all heavy atoms of the A-site and PM. For the first 0.6 ns of equilibration, the spring constants of the restraints were set to 695 pN/nm. The restraints were gradually released in ten steps of 120 ps each. Finally, all three systems were simulated at constant volume and 295 K for about 23 ns in the absence of any restraint. The root mean square deviation of each model's heavy atoms from the respective NMR coordinates is plotted in Figure S5. The RMSD values were found to saturate at approximately 3 Å within 23 ns, indicating that each structure could maintain a stable conformation. The RMSD of the free A-site complex could transiently exceed 3 Å because it contained unpaired base pairs.

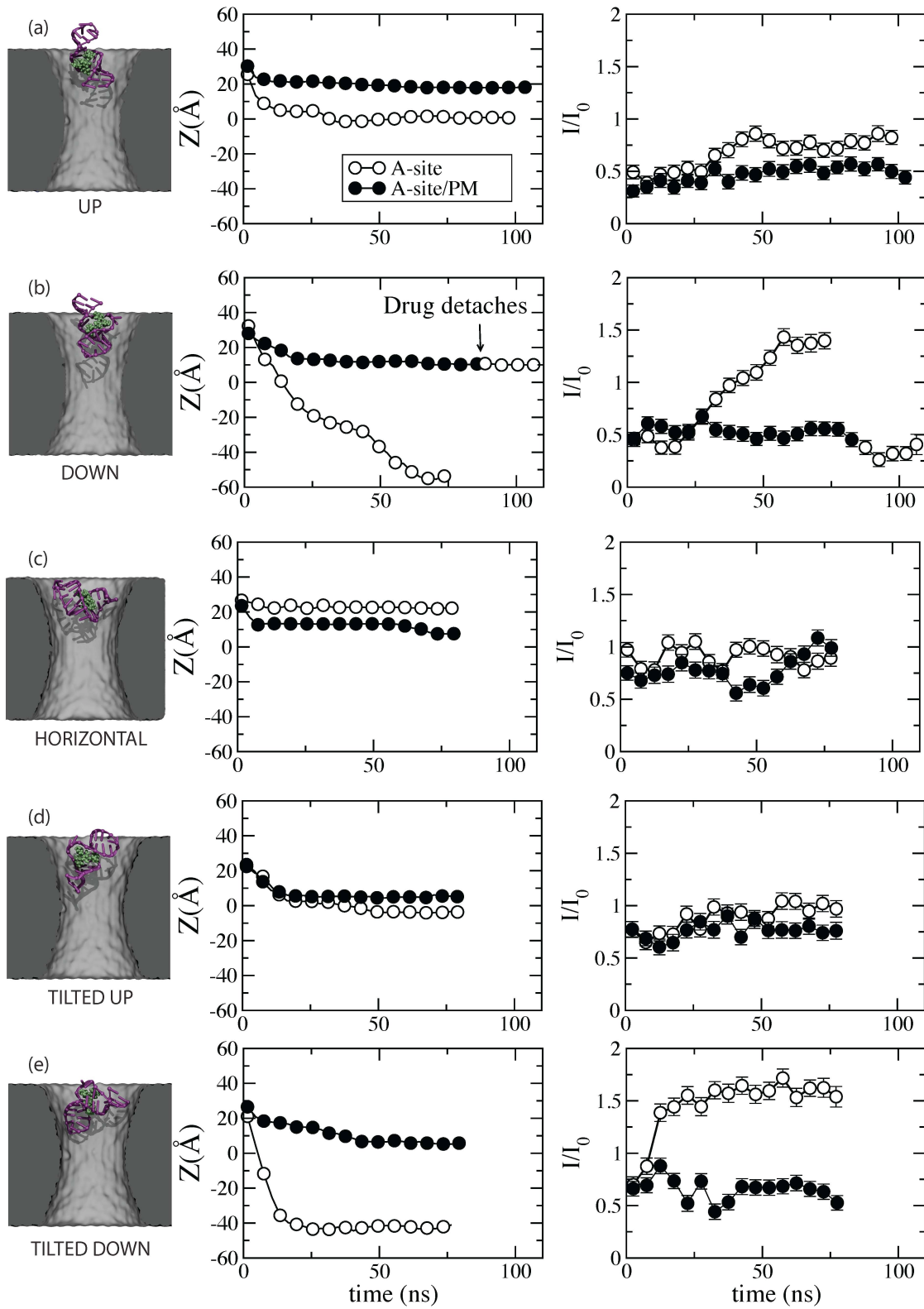


Figure S6: MD simulation of A-site translocation (with and without PM) through a 3.5-nm-diameter pore under a 300-mV bias and 273 K. The snapshots in Column I show the five initial conformations of the A-site used for these simulations. The position of the center of mass of the A-site relative to the center of the membrane is plotted versus simulation time in Column II. The snapshots in Column I are faithfully aligned with the position axis of the graphs in Column II. Column III displays the blockade current defined as the ratio of the ionic current to the open pore current at the same temperature and bias.

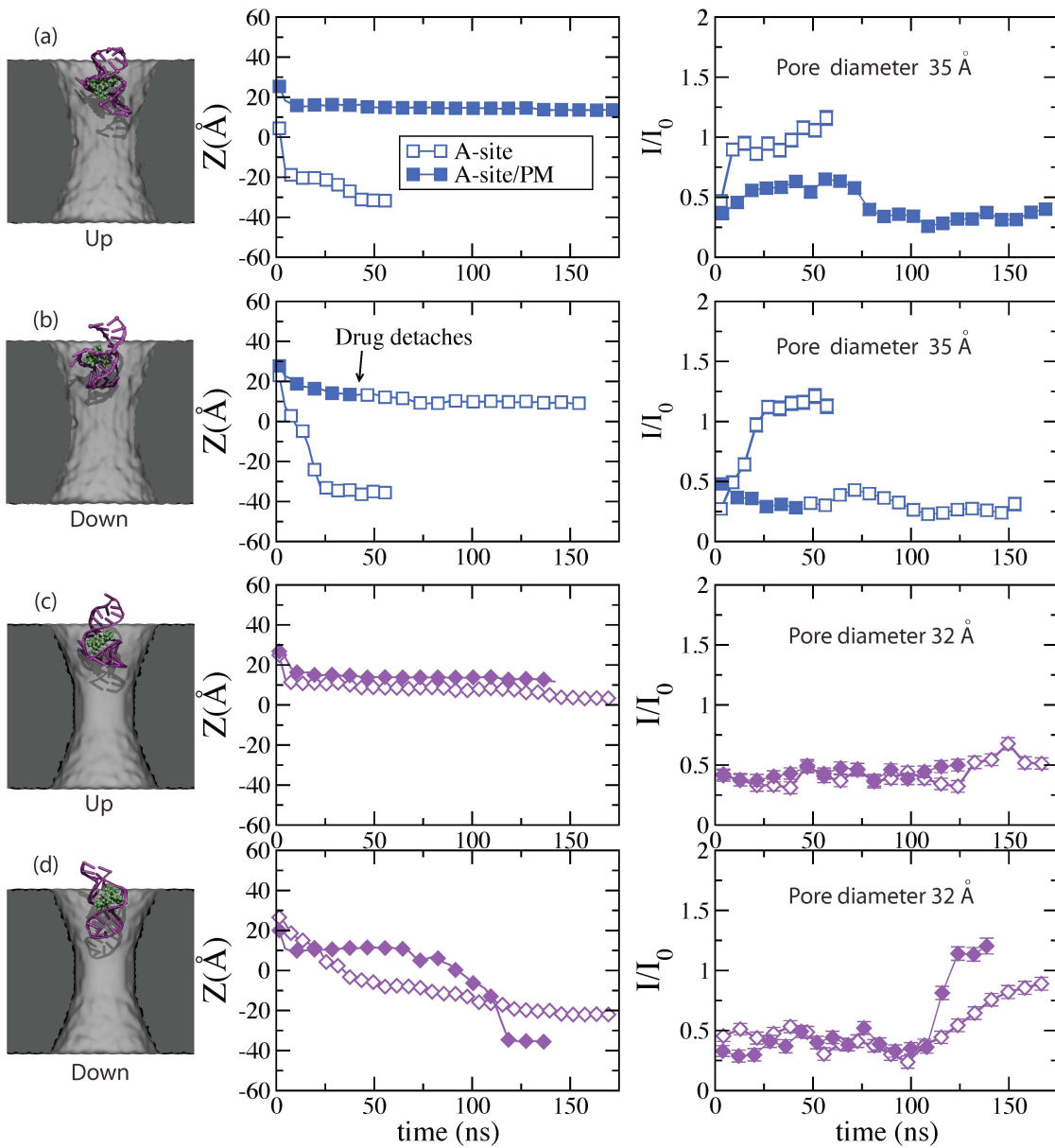


Figure S7: MD simulation of A-site translocation (with and without PM) through 3.2 (first two rows) and 3.5 (last two rows) nm-diameter pores under a 300-mV bias and 295 K. The snapshots in Column I show the initial conformations of the A-site used for these simulations. The position of the center of mass of the A-site relative to the center of the membrane is plotted versus simulation time in Column II. The data for the 3.5- and 3.2-nm-diameter pores are shown using blue squares and purple diamonds, respectively. The snapshots in Column I are faithfully aligned with the position axis of the graphs in Column II. Column III displays the blockade current defined as the ratio of the ionic current to the open pore current at the same temperature and bias.